Vehicle Trajectory Approximation and Classification

R. Fraile* and S. J. Maybank
Department of Computer Science,
The University of Reading
Whiteknights, Reading
Berkshire, RG6 6AY, UK.
[R.Fraile|S.J.Maybank]@reading.ac.uk

Abstract

We present a variational technique for finding low curvature smooth approximations to trajectories in the plane. The method is applied to short segments of a vehicle trajectory in a known ground plane. Estimates of the speed and steering angle are obtained for each segment and the motion during the segment is assigned to one of the four classes: `ahead`, `left`, `right`, `stop`. A hidden Markov model for the motion of the car is constructed and the Viterbi algorithm is used to find the sequence of internal states for which the observed behaviour of the vehicle has the highest probability.

1 Introduction

As the density of road traffic increases it becomes ever more important to detect quickly accidents or other abnormal events, both to save lives and to reduce the disruptive effects on traffic flow. Certain events can already be detected automatically using the image sequences obtained by fixed surveillance cameras which already line many motorways and main roads. These events include build ups in traffic density and vehicles coming to a halt. It is sufficient to use 2D or 'blob based' tracking provided the camera is placed high enough to avoid occlusions [4]. 2D tracking is not sufficient to recover the more detailed information needed for accurate monitoring and control of road traffic. This information can only be obtained by taking into account the 3D nature of the scene. For example, the trackers described in [5,10,11] obtain a time sequence of measurements of the 3D position of a vehicle from a monocular image sequence by matching a wire frame model of the vehicle to the images.

Once a sequence of measurements is obtained, the trajectory of the vehicle can be classified. For this we use a hidden Markov model (HMM). The method is similar to one applied successfully to speech recognition [8,9]. The measurement sequence is divided into overlapping segments. In each segment the trajectory of the car is approximated by a smooth function and then assigned to one of four categories: `ahead`, `left`, `right` or `stop`. In this way the list of segments is reduced to a string of symbols drawn from the

*Supported by DERA, Malvern, UK, under contract CSM/226

set $\{\mathtt{a}, \mathtt{l}, \mathtt{r}, \mathtt{s}\}$, where each letter corresponds to the appropriate category. The string of symbols is classified using the HMM.

2 Low Curvature Approximation

The motion of the vehicle is confined to a known ground plane, thus it is only necessary to approximate a 2D trajectory. In previous papers [6,7] vehicle motion in the ground plane was modelled by a set of stochastic differential equations driven by the tangential velocity V and the steering angle Φ. The equations are realistic in that they enforce the constraints on trajectories arising from the fact that under normal conditions a vehicle does not slip sideways. In particular, the velocity vector is always directed along the axis of the car.

The motion model assigns to each possible trajectory p of the car a cost $C_1(p)$ which is high if p has a high acceleration or a rapidly changing curvature. The trajectory carries an additional cost $C_2(p)$ which depends on the compatibility between p and the measurements. The total cost is the sum $C(p) = C_1(p) + C_2(p)$. The most likely trajectory is estimated by minimising $C(p)$ over a suitable finite dimensional space of trajectories. An expression for $C(p)$ is given in [7].

The direct estimation of the most likely or minimum cost trajectory is difficult because $C(p)$ is a highly non-linear function of p. Instead the following method for obtaining an approximation to the minimum cost trajectory is employed. Let z_i, $1 \leq i \leq n$ be the measurements of the position (x, y) of the vehicle in the ground plane obtained at times $t_1 < \ldots < t_n$ comprising one of the segments chosen from the total set of measurements. The aim is to find a trajectory $s \mapsto p(s)$ which has a low curvature and which has a low value of $\|p(t_i) - z_i\|$ for each i, $1 \leq i \leq n$. In this application the total time $t_n - t_1$ for each segment is only 1.6 s; the trajectory cannot have a complicated shape over so short a time.

Let the components of the measurements be $z_i = (z_i^x, z_i^y)$, $1 \leq i \leq n$. The x components z_i^x are approximated by a second degree polynomial

$$\hat{f}(s) = \hat{f}_0 + \hat{f}_1 s + \hat{f}_2 s^2$$

where the $\hat{f}_i$ are chosen such that

$$\sum_{i=1}^{n} (\hat{f}(t_i) - z_i^x)^2$$

is minimised. Note that a higher degree polynomial may be needed in applications where n is large and the underlying trajectory is complicated. In the current application degree two is sufficient. The z_i^y are approximated by a polynomial $\hat{g}$ in a similar way. The functions $s \mapsto \hat{f}(s)$, $s \mapsto \hat{g}(s)$ fit closely to the measurements, but in general $\hat{f}$, and $\hat{g}$ have high second order derivatives, which result in high curvatures for the ground plane trajectory $s \mapsto (\hat{f}(s), \hat{g}(s))$.

The polynomial $\hat{f}$ is replaced by a function which fits the measurements closely and which has a low second order derivative. This function is the global minimum of the functional V defined by

$$V(e) = \lambda^4 \int_{t_1}^{t_n} (e(s) - \hat{f}(s))^2 \, ds + \int_{t_1}^{t_n} \left(\frac{d^2 e}{ds^2} \right)^2 \, ds \tag{1}$$

The constant λ is determined experimentally. The value $\lambda = 62.5\,\mathrm{s}^{-1}$ is used in the experiments reported below in §5. Let f be the global minimum of V. The first integral on the right-hand side of (1) ensures that f is close to $\hat{f}$ and hence that $f(t_i)$ is close to z_i^x for $1 \leq i \leq n$. The second integral on the right-hand side of (1) ensures that f has a small second order derivative.

The Euler-Lagrange equation [1] for V is linear,

$$\frac{d^4 e}{ds^4} + \lambda^4 e = \lambda^4 \hat{f} \tag{2}$$

The polynomial $\hat{f}$ has degree two thus $e = \hat{f}$ is a solution to (2). The general solution e_m to (2) is [2]

$$\begin{aligned} e_m(s) &= \exp\left(\frac{\lambda s}{\sqrt{2}}\right)\left(a_1 \cos\left(\frac{\lambda s}{\sqrt{2}}\right) + a_2 \sin\left(\frac{\lambda s}{\sqrt{2}}\right)\right) \\ &\quad + \exp\left(-\frac{\lambda s}{\sqrt{2}}\right)\left(a_3 \cos\left(\frac{\lambda s}{\sqrt{2}}\right) + a_4 \sin\left(\frac{\lambda s}{\sqrt{2}}\right)\right) + \hat{f}(s) \end{aligned} \tag{3}$$

where the a_i are arbitrary real numbers. The expression $V(e_m)$ is a quadratic polynomial in the a_i. This polynomial is minimised, and the values of a_i at which the minimum is attained are substituted into e_m to yield f. A function g approximating to the measurements z_i^y is obtained similarly. The trajectory p defined by $s \mapsto (f(s), g(s))$, $t_1 \leq s \leq t_n$ has a low curvature and passes close to the measurements. As a result, $C(p)$ is low, where C is the cost referred to at the beginning of this section.

3 Segment Classification

Each of the measurement segments is assigned to one of the classes `ahead`, `left`, `right`, `stop`. Let $t_1 < \ldots < t_n$ be the times of the measurements in the segment of interest. As explained in §2, a smooth approximation $s \mapsto (x_s, y_s)$, $t_1 \leq s \leq t_n$ to the trajectory of the car is obtained. The least speed u of the car in the time interval $[t_1, t_n]$ is estimated by

$$u = \min\{\sqrt{\dot{x}_s^2 + \dot{y}_s^2}, t_1 \leq s \leq t_n\}$$

Let $t \in [t_1, t_n]$ be the time at which the curvature of the trajectory attains its maximum absolute value and let w be the wheelbase of the car. The greatest steering angle ϕ of the car in the time interval $[t_1, t_n]$ is estimated by

$$\phi = w \frac{\ddot{y}_t \dot{x}_t - \ddot{x}_t \dot{y}_t}{(\dot{x}_t^2 + \dot{y}_t^2)^{3/2}}$$

The quantity $\theta = u\phi/w$ is an estimate of the greatest rate of change of orientation during $[t_1, t_n]$. The segment is classified as `a`, `l`, `r` or `s` according to Table 1. The list of segments for the entire trajectory is thus reduced to a string of symbols drawn from the set $\{\mathtt{a}, \mathtt{l}, \mathtt{r}, \mathtt{s}\}$.

The next task is to find a global classification of the entire trajectory. The problem here is that the classifications for individual segments are not a reliable guide to the behaviour of the car over a long trajectory. For example, in a left turn executed over a time of several seconds many individual segments may be labelled `a` or even `r`, although the majority of the segments are likely to be labelled `l`. The classification of the global motions of the car is carried out using an HMM, as described in the next section.

class	condition
a	$-1/2 \leq \theta \leq 1/2$
l	$\theta > 1/2$
r	$\theta < -1/2$
s	$u < 1$

Table 1. Thresholds for classifying a measurement segment. The value θ is given in rad·s^{-1}, and u in ms^{-1}

4 Hidden Markov Model

As explained in [8], an HMM contains a finite set of states and a finite set of observation symbols. The state transition probability distribution is described by a matrix A with rows and columns indexed by the states. The observation symbol distribution is described by a matrix B with rows indexed by the states and columns indexed by the observation symbols. If the system is in state i, then the probability of a transition to state j is given by A_{ij}. If the system makes a transition to state j then the probability of the observation k is B_{jk}. The initial state distribution is given by a vector π indexed by the states.

The model contains four states which are in order A, L, R, S. These are the true states of the car, corresponding to ahead, turning left, turning right, stopped. They are to be inferred from the measurements. The HMM has four output symbols in order a, l, r, s. These are the symbols obtained from the measurement segments as described in §3.

The matrices A, B and the vector π are learnt from a subset of the trajectories, segmented by hand.

Figure 1. A typical image.

5 Experimental Results

This method has been tested on a set of 21 image sequences showing a car moving in a car park. The images were taken by a Canon MV1 digital video camera looking through a second floor window. A typical image is shown in Figure 1.

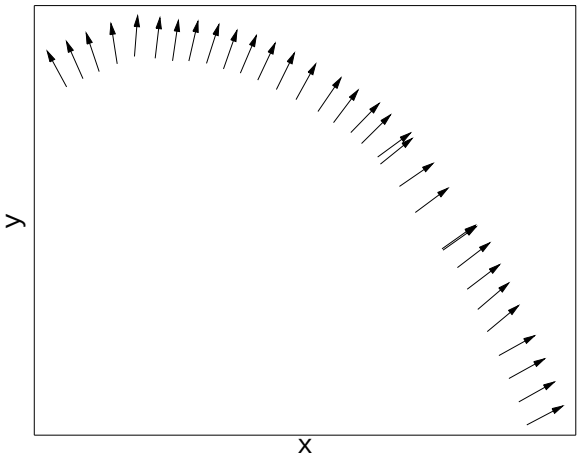

Figure 2. A left turn.

The car had a known geometrical model, and the same car was used for all the sequences. The wheelbase was $w = 2.5$ m. The camera was calibrated using the method described in [13] and measurements were obtained using the model based tracker described in [11]. The tracker measures the position (x, y) of the centre of the rear axle and the orientation θ of the vehicle. In these experiments only the (x, y) measurement was used. The angle measurements were discarded. The calibration included the determination of the ground plane position relative to the camera. The tracker was initialised by hand in the first frame of each sequence.

The sequence of measurements for each trajectory was divided into overlapping segments, each containing 10 measurements. Each pair of adjacent segments overlapped by 9 measurements. The time between the first measurement in a segment and the last measurement was 1.6 s. Experiments showed that the performance of the algorithm was degraded if the overlap between adjacent segments was reduced.

The matrices A, B and the vector π are given by

$$A = \begin{pmatrix} 111/121 & 5/121 & 3/121 & 2/121 \\ 1/32 & 31/32 & 0 & 0 \\ 5/69 & 0 & 64/69 & 0 \\ 2/63 & 2/63 & 3/63 & 56/63 \end{pmatrix}$$

$$B = \begin{pmatrix} 114/132 & 6/132 & 10/132 & 2/132 \\ 9/34 & 24/34 & 1/34 & 0 \\ 28/73 & 1/73 & 42/73 & 2/73 \\ 0 & 0 & 0 & 1 \end{pmatrix}$$

$$\pi = \left(\frac{12}{21}, \frac{1}{21}, \frac{3}{21}, \frac{5}{21}\right)^\top$$

Although the diagonal entries of B are large (for example, if the state of the car is A, then there is a high probability, 114/132, of observing the symbol a) they are not equal to 1, because there is a small probability that the observed symbol will not correspond to the true state of the car.

The probabilities in A, B, π were obtained by the hand segmentation of 21 training sequences showing the motions of a car in a car park.

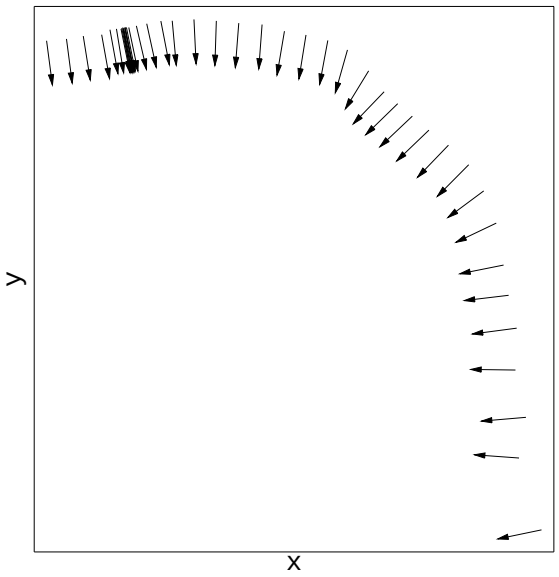

Figure 3. A right turn with a stop.

For each trajectory, the list of segments was reduced to a string of symbols using the method described in §2. The Viterbi algorithm [8] was used to calculate the sequence of possible states for which the probability of producing the observed string of output symbols was greatest.

A typical trajectory of the car is shown in Figure 2. The car moves from bottom right to top left. The arrow represents the normal to the trajectory, drawn as if the driver were extending the right arm out of the window. The base points of the arrows are the coordinates of the vehicle on each sample. The sequence of extracted symbols and the most likely sequence of states, as identified by the Viterbi algorithm, are

```
a  a  a  a  a  a  a  a  l  l  l  l  l  a  a
a  l  l  a  a  l  l  l
A  A  A  A  A  A  A  A  L  L  L  L  L  L  L
L  L  L  L  L  L  L  L
```

A more complicated trajectory is shown in Figure 3. The trajectory begins at the top left and then turns right. The sequence of observed symbols and the sequence of inferred states are

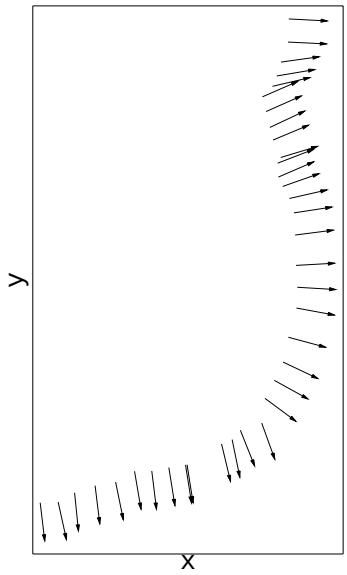

Figure 4: A more complicated trajectory.

```
s  s  s  s  s  s  s  s  s  s  s  s  s  s  s  s  r  r
a  a  a  r  r  r  r  a  a  a  a  r  r  r  r  r  r  a
S  S  S  S  S  S  S  S  S  S  S  S  S  S  S  S  R  R
R  R  R  R  R  R  R  R  R  R  R  R  R  R  R  R  R  R
```

which means that the driver stops, and then turns to the right.

A final trajectory is shown in Figure 4. The car moves from bottom left to top right. The sequence of observed symbols and the sequence of states obtained by the Viterbi algorithm are, respectively:

```
a  a  a  a  a  l  l  l  l  l  l  l  l  a  a
l  l  l  l  l  a  a  a  a  a  r  r  r
A  A  A  A  A  L  L  L  L  L  L  L  L  L  L
L  L  L  L  L  A  A  A  A  A  R  R  R
```

Some errors in the classification of the measurement segments are resolved, but others, for example at the end of the sequence in Figure 4, are not.

The entire algorithm is implemented in Mathematica [12], with a literate programming approach [3]. The functions are available at

`http://www.cvg.cs.rdg.ac.uk/~rvf/ta/`

6 Conclusions and Further Work

We have described a method for finding low curvature approximations to segments of the trajectory of a car and then using quantised data from the sequence of approximations

and a hidden Markov model (HMM) to classify the entire trajectory. The low curvature approximations are obtained only for short segments, but the approximation method can be extended to longer and more complicated trajectories.

The trajectory classification method has only been applied to a limited number of trajectories. The results suggest that HMMs can be the basis of fast and reliable algorithms for classifying trajectories and for identifying ones arising from abnormal driver behaviour. Abnormal behaviour can be learnt by the HMM in the sense that the probability of an unusual sequence of states is low.

Further work will involve extending the methods to a wider variety of vehicles and road situations. Integration of this method in a full decision system, taking into account site-dependent knowledge, such as the information given by visual traps, would have commercial applications.

References

[1] O. Bolza, *Lectures on the Calculus of Variations*, Dover (1961).

[2] J.C. Burkhill *The Theory of Ordinary Differential Equations*. University Mathematical Texts **21**, Oliver and Boyd (1968).

[3] D.E. Knuth, *Literate Programming*, Center for the Study of Language and Information, Stanford, CA (1992).

[4] D. Koller, J. Weber and J. Malik, Robust multiple car tracking with occlusion reasoning. In J.-O. Eklundh (ed.) *Computer Vision-ECCV'94*, Lecture Notes in Computer Science, **800**, pp. 189-196, Springer-Verlag (1994).

[5] H. Kollnig and H.-H. Nagel, 3D pose estimation by fitting image gradients directly to polyhedral models. *Proc. Fifth Int. Conf. on Computer Vision ICCV'95*, Cambridge, MA, pp. 569-574.

[6] S.J. Maybank, A.D. Worrall and G.D. Sullivan, A filter for visual tracking based on a stochastic model for driver behaviour. In B. Buxton and R. Cipolla (eds.) *Computer Vision-ECCV'96*. Lecture Notes in Computer Science **1065**, pp. 540-549, Springer-Verlag (1996).

[7] S.J. Maybank and A.D. Worrall Path prediction and classification based on nonlinear filtering. In G. Sommer and J.J. Koenderink (eds.) *Algebraic Frames for the Perception-Action Cycle*. Lecture Notes in Computer Science **1315**, pp. 323-343, Springer-Verlag (1997).

[8] L.R. Rabiner and B.H. Juang, An introduction to hidden Markov models, *IEEE ASSP Magazine*, Jan 1996, pp. 4-17 (1996).

[9] L.R. Rabiner, S.E. Levinson and MM Sondhi, On the application of vector quantization and hidden Markov methods to speaker-independent isolated word recognition. *Bell System Tech. J.* **62**, pp. 1075-1105 (1983).

[10] G.D. Sullivan, Visual interpretation of known objects in constrained scenes. *Phil. Trans. R. Soc. Lond., Series B*, **337**, pp. 361-370 (1992).

[11] G.D. Sullivan, Model-based vision for traffic scenes using the ground plane constraint, In D. Terzopoulos and C. Brown (eds.) *Real-time Computer Vision*, CUP (1994).

[12] S. Wolfram, *The Mathematica Book*, 3rd edition, CUP (1996).

[13] A.D. Worrall, G.D. Sullivan and K.D. Baker A simple intuitive camera calibration tool for natural images. In E. Hancock (ed.) *British Machine Vision Conference 1994*, **2**, pp. 781-790 (1994).